ELSEVIER

Desalination 170 (2004) 281–308

DESALINATION

www.elsevier.com/locate/desal

A comprehensive review of nanofiltration membranes: Treatment, pretreatment, modelling, and atomic force microscopy

N. Hilal[a*], H. Al-Zoubi[a], N.A. Darwish[b], A.W. Mohammad[c], M. Abu Arabi[d]

[a]*Advanced Water Treatment Group, School of Chemical, Environmental and Mining Engineering, The University of Nottingham, NG7 2RD, United Kingdom*
Tel. +44 (115) 951-4168; Fax: +44 (115) 951-4115; email: nidal.hilal@nottingham.ac.uk
[b]*Department of Chemical Engineering, College of Engineering, Jordan University of Science and Technology, PO Box 3030, Irbid, Jordan*
[c]*Department of Chemical and Process Engineering, Universiti Kebangsaan Malaysia, 43600 UKM Bangi, Selangor Darul Ehsan, Malaysia*
[d]*The Middle East Desalination Research Centre, PO Box 21, Al Khuwair, Postal Code 1333, Oman*

Received 12 November 2003; accepted 5 January 2004

Abstract

Nanofiltration membranes (NF) have applications in several areas. One of the main applications has been in water treatment for drinking water production as well as wastewater treatment. NF can either be used to treat all kinds of water including ground, surface, and wastewater or used as a pretreatment for desalination. The introduction of NF as a pretreatment is considered a breakthrough for the desalination process. NF membranes have been shown to be able to remove turbidity, microorganisms and hardness, as well as a fraction of the dissolved salts. This results in a significantly lower operating pressure and thus provides a much more energy-efficient process. Similar to other membrane processes, a major problem in NF membrane applications is fouling. Several studies have investigated the mechanisms of fouling in NF membranes and suggested methods to minimize and control the fouling of NF membranes. For NF membrane characterizations and process prediction, modeling of NF processes and the use of atomic force microscopy (AFM) are very important. The ability to predict the performance of NF processes will lead to a lower number of experiments, saving of time and money, and help to understand the separation mechanisms during NF. A comprehensive review of NF in water treatments is presented including a review of the applications of NF in treating water as well as in the pretreatment process for desalination; the mechanism as well as minimization of NF membrane fouling problems; and theories for modelling and transport of salt, charged and noncharged organic compounds in NF membranes. The review will also address the application of AFM in studying the morphology of membrane surfaces as part of the NF membrane characterization.

Keywords: Nanofiltration; Pretreatment; Fouling; Modeling; Atomic force microscopy; Desalination

*Corresponding author.

doi:10.1016/j.desal.2004.01.007

1. Introduction

The nanofiltration (NF) membrane is a type of pressure-driven membrane with properties in between reverse osmosis (RO) and ultrafiltration (UF) membranes. NF offers several advantages such as low operation pressure, high flux, high retention of multivalent anion salts and an organic molecular above 300, relatively low investment and low operation and maintenance costs. Because of these advantages, the applications of NF worldwide have increased [1]. The history of NF dates back to the 1970s when RO membranes with a reasonable water flux operating at relatively low pressures were developed. Hence, the high pressures traditionally used in RO resulted in a considerable energy cost. Thus, membranes with lower rejections of dissolved components, but with higher water permeability, would be a great improvement for separation technology. Such low-pressure RO membranes became known as NF membranes [2]. By the second half of the 1980s, NF had become established, and the first applications were reported [3,4].

This paper reviews several aspects of NF membranes such as the applications in treatment of ground, surface, and wastewater; as a pretreatment for desalination, fouling, and the separation mechanism; and modelling of NF membranes. In addition, the application of atomic force microscopy (AFM) in studying the morphology of the NF membrane surfaces will also be reviewed.

2. NF membranes in water treatments

In addition to having the capability to reduce the ionic strength of the solution, NF membranes can remove hardness, organics and particulate contaminants. Many researchers have used NF to achieve those objectives and the following sections highlight their major findings.

2.1. Ground water

The softening of ground water using NF has been studied by many investigators [4–8]. Schaep et al. [4] used several different types of NF membranes for hardness removal. Retentions higher than 90% were found for multivalent ions, whereas monovalent ions were retained for about 60–70%. Sombekke et al. [5] compared NF membranes with pellet softening and granular activated carbon for softening water. Both methods gave good results; however, NF membranes have several advantages from the point of view of health aspects and lower investment costs. Removal of natural organic matter (NOM) and disinfection by-product (DBP) precursors were also studied [9–16]. Jacangelo et al. [11] reported that both RO and NF are used in the US for removal of NOM. To date, NF has been employed primarily for groundwater containing relatively low total dissolved solids but with high total hardness, color, and DBP precursors. Escobar et al. [12] found that the rejection of assimilable organic carbon was greater than 90% at pH 7.5 and greater than 75% at pH 5.5 by using TFC-S NF membranes.

The removal of pesticides and some micropollutants from ground water has been studied by many researchers [17–25]. Van der Bruggen et al. [17] showed that the NF70 membrane can reject pesticides such as atrazine, simazine, diuron and isoproturon over 90%. Similarly, removal of trichloroethylene and tetrachloroethylene can be achieved using several different types of NF membranes [25].

Kettunen and Keskitalo [26] studied the removal of fluoride and aluminum from groundwater sources in Finland. In addition to the removal of hardness, nitrates, iron and strontium, fluoride removal was also mentioned by Pervov et al. [27]. The removal of dissolved uranium from natural waters has been conducted by Raff and Wilken [28]. The multivalent anion complexes of uranium were rejected to about 95%. Finally, arsenic removal and the effect of pH in the rejection process were studied by Urase et al. [29]. It was shown that the rejection of arsenite

As(III) increased with the increase of pH from 50% at pH 3 to 89% at pH 10,while the degree of increase with As(V) was smaller; from 87% at pH 3 to 93% at pH 10.

2.2. Surface water

Surface waters often have a changing chemistry or composition due to seasonal changes or after dilution with rain. NF is a reliable option for surface water treatment, although the focus is here rather on removal of organics than on softening [2]. Hardness removal from a lake in Taiwan has been studied by Yeh et al. [30] using different methods such as a conventional process followed by ozone, GAC and pellet softening, and an integrated membrane process (UF/NF) and the conventional process. Softening was achieved by all processes, but water produced by the membrane process had the best quality as measured by turbidity (0.03 NTU), total hardness rejection (90%), and dissolved organics rejection (75%).

Removal of DBP precursors and NOM from surface water sources has been studied by many investigators [31–35]. Visvanathan et al. [32] studied the effect of the presence of ions, operating pressure, feed, pH, and suspended solids on rejection properties, and concluded that higher pressure and suspended solids content increase rejection, while rejections are somewhat lower at higher ionic strength. Also, they conclude that both high and low pH of the feed water produce low rejection, while better rejection has been found at a pH range of 7–9, which indicates that pH adjustment of the feed may not be required.

Removal of organic micropollutants was also investigated by other researchers [36,37]. Koyuncu and Yazgan [37] had good results in treating salty and polluted water from Kucukcekmece Lake in Istanbul using the TFC-S NF membrane. NF membranes were also found to be able to remove viruses and bacteria from surfaces quite successfully [11,38–41]. Reiss et al. [42] used an integrated membrane system of microfiltration with NF to remove *Bacillus subillus* spores from 5.4 to 10.7 log. Using a novel NF membrane (NF 200), removal of organics (up to 96%) in a large NF plant in Paris [43,44] was achieved. NF has been also used to remove both arsenic(V) and arsenic(III) from surface water [45–48]. These studies showed that (using NF membranes) the rejection of As(V) is relatively high, up to 90%, while As(III) is just around 30%.

An investigation of the rejection of alkyl phthalates using four types of NF membranes was conducted by Kiso et al. [49]. Monovalent ions, like nitrates, however, were found to have a lower extent of rejection by NF membranes [19,50–52]. Molinari et al. [53] compared rejection of several pollutants such as silica, nitrate, manganese and humic acids by means of RO and NF membranes. At a pH of 8, RO rejected silica, NO^{3-}, Mn^{2+}, and humic acid in a rate equal to 98%, 94%, 99% and 95.5%, respectively, while NF had a much lower rejection, i.e., 35%, 6%, 80% and 35%, respectively. Sulfate could be removed from chloralkali plant brine streams by NF [54]. The results showed that the NF membranes effectively rejected SO_4^{2-} up to 95% in concentrated brines.

2.3. Wastewater

NF is an efficient and ecologically suited technology for decontamination and recycling of wastewater generated in many industries. Afonso and Yafiez [55] used NF to treat fish meal wastewaters. NF reduced the organic load in the wastewaters and promoted their partial desalination, making water reuse possible. A major problem of the wastewater treatment is the water recovery rate, which should be close to 100%. To achieve this target, many researchers investigated an integrated membrane system [56–59]. Rautenbach and Linn [56] and Rautenbach et al. [57] used a new concept of integrated membranes consisting of RO/NF/high-pressure RO. The integration can achieve water recovery rates of

more than 95% in the case of dumpsite leachate, which promises an almost zero discharge process. Hafiarle et al. [60] investigated the removal of chromate, from water using a TFC-S NF membrane as a possible alternative to the conventional methods of Cr(VI) removal from an aqueous solution. The results showed that the rejection depended on the ionic strength and pH. Better retention was obtained at basic pH (up to 80% at a pH of 8). Results also showed that NF is a very promising method of treatment for wastewater charged with hexavalent chromium. The same membrane was used by Koyuncu [61] to treat opium alkaloid processing industry effluents.

Application of NF in the treatment of textile wastewater was conducted by many researchers [62–65]. Tang and Chen [62] used NF to treat textile wastewater which was highly colored with a high loading of inorganic salts. At an operating pressure of 500 kPa, the flux obtained was very high, while the rejection of dye was 98% and the NaCl rejection was less than 14%. Thus, a high quality of reuse water could be recovered. On the other hand, Voigt et al. [64] suggested a new TiO_2-NF ceramic membrane to decolor textile wastewater using an integrated pilot plan. The results show that it is possible to clean colored wastewater with dye retention varying from 70% to 100%, COD reduction of 45–80%, and salt retention of 10–80%. A new ceramic K-NF membrane was studied by Webar at al. [65] with almost the same results as that of the TiO_2-NF membrane.

Jakobs and Baumgarten [66] showed that NF could remove lead up to 90% from a nitric acid solution. Also, purification of phosphoric acid by NF (DS5DL NF) was studied [67] using different commercial membranes of common industrial use. The results show that the rejection of impurities is around 99.2%.

3. NF as pretreatment for desalination

Feed pretreatment is one of the major factors determining the success or failure of a desalination process. Different methods of pretreatment for desalination process were suggested by many researchers. Traditional pretreatment is based on mechanical treatment (media filters, cartridge filters) supported by extensive chemical treatment [68]. In the past, conventional pretreatment (i.e., coagulation, flocculation, acid treatment, pH adjustment, addition of anti-scalant and media-filtration) was usually used [69]. The main problem in using conventional pretreatment is corrosion and corrosion products. For example, in the acid dosing system, corrosion of metallic surfaces and corrosion products will roughen the surface of the equipment, which provides active sites for precipitation of more scale deposits [69,70]. In addition, this pretreatment is known to be complex, labor intensive and space consuming [71].

Pressure-driven membrane processes [microfiltration (MF), ultrafiltration (UF), and NF] are the new trends in designing a pretreatment system. The introduction of NF as a pretreatment will lead to a breakthrough in the application of RO and MSF because it has implications for the desalination process itself, and not only on quantity of the feed water [68]. MF can remove suspended solids and lower the silt density index (SDI) while in UF, not only suspended solids and large bacteria are retained, but also (dissolved) macromolecules, colloids and small bacteria. Redondo [72] strongly preferred MF or UF as a pretreatment over conventional pretreatment to treat difficult effluent water.

Bou-Hamad et al. [73] tested three pretreatment methods (conventional, a beachwell seawater intake system, and MF) prior to RO. According to the results of SDI, COD and BOD removal and the total unit cost, the beachwell seawater intake and MF systems were identified as promising techniques to replace conventional pretreatment. However, all of the pretreatments mentioned did not lower the TDS value.

Several studies have also been carried out on the use of UF membrane as pretreatment [70,71,

74,75]. Van Hoop et al. [74] concluded that UF can provide a feed water quality with a SDI below 2, and operational costs were very attractive. The same results were obtained by Al-Ahmad and Adbul Aleem [70], who concluded that the hollow-fiber UF process promises to be a simple, easy-to-use, and robust alternative to the cumbersome conventional forms of pretreatment. The surface seawater SDI of 13–25 was reduced below 1 by UF, whereas conventional pretreatment failed to reduce it below 2.5 [75]. The UF pretreatment also provide filtered water with high and constant quality that enhanced the reliability of the RO desalination plant. Teng et al. [76] compared the use of UF and MF as a pretreatment. The results show that the higher operating flux of the MF pilot system was achieved at the expense of increasing transmembrane pressure, which had to be kept constant. However, the SDI of the filtrate produced by the UF pilot system was superior to that produced by the MF pilot system. In general, the filtrate quality of the MF system was inferior to that of UF pilot system.

Recently, Vail and Doussau [77] conducted a pilot test using a new 0.1 μm Microza hollow-fiber MF membrane as a pretreatment to RO on Mediterranean seawater. A pilot rig was operated at different fluxes ranging from 80 to 140 l/h.m^2 with and without ferric chloride addition. During the test, the microfilter water SDI remained below 2 under the optimized operating conditions. Longer runs between chemical cleaning and better filtered water quality were obtained with ferric chloride addition to the raw seawater and by performing backwashes with sodium hypochlorite. Again, the same membrane underwent pilot tests at three different locations on Mediterranean seawater [78]. The same results were obtained by the membrane, which provided clarified water to RO having a SDI of 1.8 or less, which allows RO operation at higher recovery, enhancing the total system running cost.

The Caspian Sea in Russia is characterised by having low TDS but a relatively high boron content (4–5 ppm), which exceeds the hygienic standards in Russia (0.4–0.5 ppm). To achieve the needed removal of boron, Pervov et al. [79] suggested a technological scheme including clarification, acid and antiscalant dosage as a pretreatment, and double-stage RO with caustic dosing into the first stage product.

NF was used for the first time by Hassan et al. [80] as pretreatment for seawater reverse osmosis (SWRO), multistage flash (MSF), and seawater reverse osmosis rejected in multistage flash ($SWRO_{rejected}$–MSF) processes. In these integrated processes, NF minimized hardness, microorganisms and turbidity. At a pressure of 22 bar, NF removed hardness ions of Ca^{2+}, Mg^{2+}, SO_4^{2-}, HCO_3^-, and total hardness by 89.6%, 94.0%, 97.8%, 76.6% and 93.3%, respectively. In addition, NF reduced the monovalent ions of Cl^+, Na^+, and K^+; each ion was separated by 40.3% and overall seawater TDS by 57.7%, while the total hardness was removed by 93.3%. The permeate thus obtained was far superior to seawater as a feed to SWRO or MSF. This made it possible to operate a SWRO and MSF pilot plant at a high recovery: 70% and 80%, respectively.

The integration of NF with MSF processes makes it possible to operate MSF plants on NF-product or $SWRO_{rejected}$ from a NF–SWRO unit at a high distillation temperature of 120°C to 160°C with high distillate recovery, and again without chemical addition. Thus, MSF and NF–$SWRO_{rejected}$–MSF could be operated at a top brine temperature of 120°C without any scaling problems [81]. These integrated desalination systems, combined with a reduction of chemicals and energy, allows producing fresh water from seawater at a 30% lower cost compared to conventional SWRO [82].

NF pretreatment of seawater in desalination plants: (1) prevented SWRO membrane fouling by the removal of turbidity and bacteria, (2) prevented scaling (both in SWRO and MSF) by removal of scale forming hardness ions and (3) lowered required pressure to operate SWRO

plants by reducing seawater feed TDS by 30–60%, depending on the type of NF membrane and operating conditions.

Later, a demonstration plant was built at Umm Lujj, Saudi Arabia, consisting of six spiral-wound NF modules (8×40") followed by three SWRO elements [83]. The results obtained from the demonstration unit confirmed the above results obtained from the pilot plant study. Criscuoali and Drioli [84] concluded that the introduction of NF for water pretreatment leads to an improvement in the performance by maintaining almost invariant the energy requirement. Mohsen et al. [85] investigated NF to treat brackish water collected from Zarqa basin, Jordan. The results show than NF is efficient for reducing the organic and inorganic contents and gives a high water recovery up to 95%. Pontie et al. [86] studied the possibility of obtaining a partial demineralization of seawater using two successive NF stages. The treated water (salinity 9 g/L) could be used in the field of human health (i.e., preparation of nasal sprays, medical dietetics and hot mineral springs).

Recently, several different types of integrated membranes were used as a pretreatment to desalination. Drioli et al. [87] introduced membrane distillation (MD) to treat the RO brine. This enhanced the recovery factor of RO. Using the newly integrated MF/UF+RO+MD, the preliminary experimental results confirmed the possibility of reaching a seawater recovery factor of 87%. Ohaa et al. [88] proposed an integrated system for the complete usage of components in seawater with a high recovery of water up to 90% as shown in Fig. 1. Another integrated system (NF+RO+MC) was suggested by Drioli et al. [89] where MC is a membrane crystallizer. MC was used to achieve the total recovery of desalted water. The presence of the NF in this integration allowed an increase in the water recovery of the RO unit up to 50%. Moreover, introduction of a MC led to a 100% recovery and elimination of the brine disposal problem, representing the pure crystals produced as a valuable product. The most important maintenance problem associated with RO operation is the membrane fouling, especially biological fouling (biofouling).

Visvanathafl et al. [90] used a membrane bioreactor (MBR) as a pretreatment process to eliminate this biofouling. MBR is the process in which a conventional biological system is coupled with the membrane process (MF or UF). The results show that the MBR system produced better effluent with 78% DOC removal, and the filtrate yielded the highest permeate flux improvement, which was approximately 300% compared with non-pretreated seawater. A hybrid NF/RO/MSF crystallization system offered very promising performance: high water recovery (77.2%) and water costs as low as \$0.37/m^3 were suggested by Turek and Dydo [91].

4. Membrane fouling

Membrane fouling is caused by dissolved inorganics ($BaSO_4$, $CaCO_3$) or organic components (humic acids), colloids (suspended particles), bacteria or suspended solids [92,93]. Fouling may occur in pores of membranes by partial pore size reduction caused by foulants adsorbing on the inner pore walls, pore blockage and surface fouling such as cake and gel layer formation [94]. Fouling will lead to higher operation costs: higher energy demand, increase of cleaning and reduced life-time of the membrane elements [95]. Existing fouling indices to measure the colloidal fouling potential of feedwater are the SDI, applied worldwide, and the Modified Fouling Index (MFI). Both tests are designed to simulate membrane fouling by feeding water through a 0.45 μm microfilter in dead-end flow [96].

The formation of a membrane fouling layer was monitored during the treatment of polluted surface water using spiral-wound NF membranes [97]. The plant feed was not disinfected and

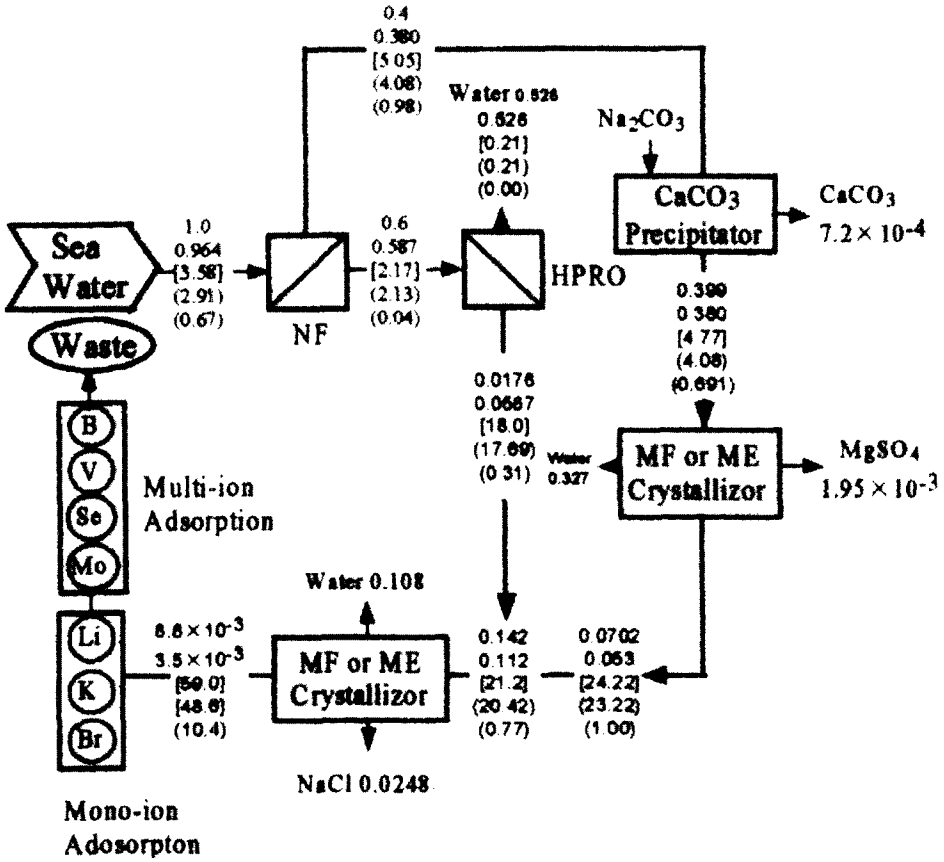

Fig. 1. Weight and composition of each process stream in the case of 90% recovery of desalted water, using an HPRO system for NF scale removal (based on 1 kg of raw seawater). Total weight, kg; water weight, kg; mono and multivalent ion, wt% (monovalent ion, wt%; multivalent ion, wt%) [88].

displayed a high fouling tendency. The fouling layer was shown to be a mixture of biological, organic and inorganic species. Calcium and phosphate were the main inorganic compounds present with minor amounts of iron and aluminum. The high level of phosphorus found was probably due to the use of sodium hexametaphosphate as a pretreatment agent (Table 1).

Boerlage et al. [96] developed a MFI using UF modules as a water quality indicator and to predict flux decline occurring in membrane filtration installations. The MFI–UF was found to be a promising tool for measuring the colloidal fouling potential for RO nano- and UF systems.

Table 1
Concentration of various elements in the fouling layer [97]

Element	Concentration $\mu g/cm^2$ membrane area
Calcium	41.9
Phosphorus	32.2
Sulphur	2.6
Magnesium	1.6
Iron	17.5
Organic carbon	13.7

The extent to which UF membranes are capable of retaining colloidal particles depends on the UF pore size expressed as a molecular cut-off (MWCO), surface morphology (e.g., porosity) and the nature of the membrane material (e.g., hydrophilicity). These UF membrane properties also influence the filtration mechanisms occurring during the test (e.g., cake and blocking filtration). Therefore, the influence of UF membrane properties on the MFI–UF was examined to explain the occurrence of filtration mechanisms in the test. The MFI–UF test may be equally applied for flux decline prediction and a differential pressure increase in NF and UF to determine the backwash frequency of a feed water.

Biofouling — defined as accumulation of microorganisms, i.e., biofilm on a surface by growth and/or deposition at such a level that causes operational problems — is difficult to identify. It may cause problems such as declined normalized flux and/or increased normalized pressure drops during NF or RO [93]. Controlling biofouling can be achieved by (1) far-reaching removal of degradable components from the feedwater, (2) securing the purity of the chemicals dosed, and (3) performing effective cleaning procedures. Also a cleaning procedure applied when fouling is not a problem might delay biofilm formation.

Vrouwenvelder and Kooij [98] showed that the diagnosis of the type/cause of fouling is an essential first step to controlling further fouling. A quick scan (autopsy) gives conclusive information about the types and extent of fouling of the membrane filtration plant. This opens ways for prevention and control of fouling. The tools (AOC-test, Biofilm monitor) can be used to test chemicals dosed on the risk of (bio)fouling. In addition, Vrouwenvelder et al. [95] made an overview for coherent tools for fouling of NF and RO membranes. These tools — developed for the diagnosis, prediction, prevention, and control of fouling — have been applied in practice and have proven their value in controlling fouling. An overview is shown in Table 2 [95].

The specific oxygen consumption rate is a (SOCR) parameter for determining the presence of an active biomass in a membrane system by measuring the oxygen demand, while ScaleGuard is a continuous on-line monitor with a single spiral-wound membrane element that detects scaling in an early stage when fed with the concentrate from either a pilot or full-scale plant. Scaling was observed on the ScaleGuard before it occurred on the full-scale installation.

The presence of calcium and humic substances or NOM in surface waters can cause severe fouling of NF membranes [99]. It was found that at high calcium concentrations fouling is detrimental, with the mechanism depending on solution chemistry. Calcium–humate complexes caused the highest flux decline due to their highly compactable floc-like structure compared to calcite precipitates. Deposition of calcium and organics increased with pH due to the precipitation of calcite and adsorption of organics on the calcite surface. Humic acid caused the highest flux decline of the three organics used due to its highest concentration in the boundary layer, which was related to its largest molecular weight and thus a lower diffusion away from the membrane. As a result, precipitation occurred. Operation at low flux, low transmembrane pressure and high shear reduced the deposition of insoluble matter at the membrane surface and thus fouling.

In a more detailed study, Hong and Elimelech [100] investigated the role of chemical and physical interactions in NOM fouling of NF membranes. The role of solution ionic strength, pH, and divalent cations in NOM membrane fouling, as well as the fouling mechanisms involved, are reproduced in Fig. 2 [100]. Of these chemical factors, the presence of divalent cations such as calcium and magnesium had a marked effect on NOM fouling. In addition, it was shown

Table 2
Overview of tools available for determining the fouling potential of feed water and fouling diagnosis of NF and RO membranes used in water treatment [95]

Tools	Fouling diagnosis	Comment
Integrated diagnosis (autopsy)	Biofouling, inorganic, compounds and particles	Diagnosis of foulant in membrane elements
Biofilm monitor and AOC	Biofouling	Predictive and prevention of biofouling by determining the (growth) potential of water
SOCR	Biofouling	Non-destructive method for determining active biomass in membrane systems
MFI-UF	Particulate	Particulate fouling potential of water
ScaleGuard	Scaling	Optimizing recovery, acid dose and anti-scalant dose

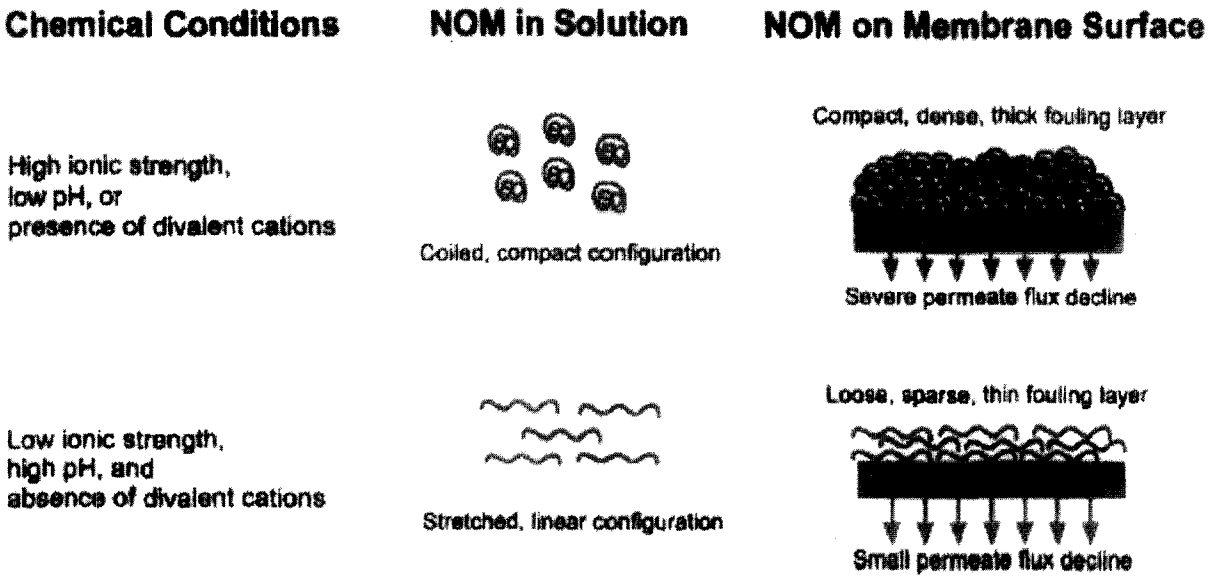

Fig. 2. Schematic description of the effect of solution chemistry on the conformation of NOM macromolecules in the solution and on the membrane surface, and the resulting effect on membrane permeate flux. The NOM fouling described in the diagram is applicable for permeation rates above the critical flux. The difference between the two chemical conditions shown becomes less clear at very high permeate flux. At low permeate flux (below the critical flux), no significant fouling is observed for both conditions [100].

that rapid membrane fouling occurs at high permeation rates, even under chemical conditions not favorable for fouling, such as low ionic strength, low levels of divalent cations, and high pH. The rate of fouling is controlled by an interplay between permeation drag and electrostatic double

layer repulsion; that is, NOM fouling of NF membranes involves interrelationship (coupling) between physical and chemical interactions. Also, the addition of a strong chelating agent (EDTA) to feed water reduces NOM fouling significantly by removing free and NOM-complexed calcium ions.

A more negatively charged membrane surface correlated with increased fouling, indicating electrostatic repulsion, was not effective for fouling control. Increased surface area due to greater surface roughness for the more negatively charged membranes may have contributed to organic adsorption fouling. Fouling was reduced with addition of monochloramine, lower flux, and lower recovery. Experiments operated under such conditions did not produce fouling and affirmed the viability of integration membrane systems (IMSs) for treatment of this source [42].

The effect of membrane fouling on rejection was presented by Schafer et al. [94]. The study was based on experiments with MF, UF, and NF membranes. It was concluded that fouling was dependent on pore size and was caused by large colloids (250 nm) or coagulant flocs in MF, small colloids, organic-calcium flocs and aggregates with a dense structure (formed slowly) in UF, and by a calcium-organic precipitate in NF. The fouling influenced the rejection of colloids in MF and that of NOM in UF and NF. If a highly charged layer were deposited on NF membranes, cation rejection was also influenced. The characterization of permeate organics revealed that low molecular weight acids passed through the NF membranes and that the rejection of these acids was also dependent on the deposit on the membrane.

The mechanisms which can explain such an increase in rejection are different for the three membrane processes. In MF, pore plugging and cake formation was found responsible for fouling. This reduces the pore size and increases rejection. In UF, internal pore adsorption of calcium-organic flocs reduces the internal pore diameter and subsequently increases rejection. In NF, the key factor appears to be the charge of the deposit. This was investigated with the deposition of a ferric chloride precipitate. If the precipitate were a high positive charge, the rejection of cations increased and that of negatively charged low molecular weight acids decreased compared to more neutral or negative precipitates. In essence, the rejection characteristics of membranes depended more on the fouling state of the membranes and the nature of foulants than on the initial membrane characteristics. On the other hand, Kosutic and Kunst [101] concluded that the pore size distribution curves and effective number of pores on the membrane surface indicated plugging of the tight network pores in the membrane surface and even their disappearance during prolonged fouling. The negligible changes of the the NF membrane performance parameters during membrane fouling with humic acid could be attributed to insignificant changes in the pore size distribution and the effective number of pores in the surface of the membrane. A delay of chemical cleaning of the fouled membrane led to irreversible changes in the porous structure of both the RO and NF membranes, which were caused by microbial activity.

Depending on the feed composition, flux decline ranging from a few percent to a complete loss of water flux can be found. For aqueous solutions containing organic components, in the absence of suspended solids or high concentrations of ions that may cause scaling, adsorption of organic material on the membrane surface is the major fouling mechanism [92]. Identification of the parameters that play a role in the process of adsorption on the membrane surface should lead to a better understanding of the mechanism that results in a hindrance of the water flux, and eventually to pore blocking. In that study, many parameters were selected for a detailed investigation of the adsorption process such as dipole moment, polarizability, dielectric constant, solubility in water, octanol–water partition coeffi-

cient, contact angle membrane/water, molecular size, and pKa. All of these parameters were evaluated in the framework of adsorption on NF membranes from an aqueous solution. The use of each parameter for describing adsorption was discussed. The pKa was rejected on theoretical grounds; other parameters such as the solubility in water proved to be impractical. Eventually, the dipole moment, octanol–water partition coefficient, and molecular size were selected.

The adsorption of organic molecules from an aqueous solution on the membrane surface or inside the membrane pores has a large influence on water flux. The more a given component is adsorbed on the membrane, the larger the flux decline. This may be up to a flux decline of 60% for a concentration of 10 mmole/l of a single organic component in pure water. Schaep et al. [4] suggested UF as pretreatment, adding hydrochloric acid to minimize the fouling, especially to prevent calcium carbonate. Finally, Shaalan [102] suggested an empirical equation to predict the impact of some water contaminants on flux decline of the NF membranes. These formulae enable decision-making concerning the suitable pretreatment for NF schemes and also selection of the most appropriate cleaning cycle. The correlation [Eq. (1)] is applicable for the following conditions: t (time) = 10–80 h, I (ion strength)= 1.6–75 mM, TOC concentration = 0–20 mg/l, P (operating pressure) = 80–147 psi and d (membrane cutoff) = 300–1000 Dalton. This correlation can give a reasonable prediction of flux decline changes with respect to an initial set of conditions:

$$J/J_0 = 0.65 \exp(-0.13t) \exp(-0.031I) \exp(0.896\,\mathrm{TOC}) \exp(1.23P) \exp(-0.34d) \quad (1)$$

5. Separation mechanism with NF membranes

NF combines removal of uncharged components at nanoscale with charge effects between solution and the surface of the membrane. The removal of uncharged components results from size exclusion or may be a result from differences in diffusion rates in a non-porous structure, which depend also on molecular size [2]. The charge effect, on the other hand, results in removal of (mainly multivalent) ions; the former effect results in the removal of uncharged organic species. Thus, the separation performance of NF membranes can be identified into the sieving (steric-hindrance) effect and Donnan (electrostatic) effect [103].

Kosutic and Kunst [104] showed that the rejection of organics depended on the sieving parameters (solute and pore size). In addition to that factor, Van der Bruggen et al. [105] concluded that the polarity and the charge of organics might influence the rejection process, especially when the pore sizes of membranes are large. The molecular diffusion is another factor affecting the rejection as mentioned by Chellam and Taylor [106]. The rejection of ionic components in NF occurred as a result of charge interactions between the membrane surface and the ions (Donnan exclusion). High retentions were found for Na_2SO_4 and for $MgCl_2$ while the retention for NaCl was much lower [107]. Lhassani et al [108] suggested that ions are transferred by two mechanisms in NF: (1) convection: the larger ions are more retained (physical parameters); (2) solubilization–diffusion: a function of the solvation energies and the partition coefficient. The larger the ion, the less well it is retained (chemical parameters). A pilot plant was built to remove the ions of the same valences (fluoride, bromide, and chlor-ide ions). The results indicated that the smaller the ion, the better it is retained, mainly at low pressure, when chemical selectivity predominates. This is derived from the solvation energy of the ions by water. Since fluoride ions are more solvated, they are better retained than chloride and iodide ions.

Schaep and Vandecasteele [109] used three methods to determine the charge of NF mem-

branes. The methods were: titration, streaming potential, and membrane potential. The results of the membrane potential measurements, where a membrane separates two electrolyte solutions, were in qualitative accordance with the results of titration. It was shown that ion diffusion is influenced by the membrane charge, and anion diffusion through negative membranes is more hindered than cation diffusion, while the opposite is found for positively charged membranes. The enhanced Donnan effect on rejection of mixture of polyelectrolyte and monovalent salt (NaCl) using two NF membranes was studied [110].

The retention of Na^+ and Mg^{2+} ions in their nitrate solutions was studied in the pH range of 0.5 to 7.0 using a NF membrane [111]. It was shown that the Mg^{2+} ions were very well retained (97.5–99.5%) within that pH range, while the retention of the Na^+ ion varied from 80% to 40%. The small Na^+ retention was measured in neutral conditions. In addition, it seems that at very low pH the membrane loses most of its charge due to a high concentration of protons. This enables the separation of cations, mainly by their size characteristics. Afonso et al. [112] suggested a relationship between the effective surface charge (C_M) of two NF membranes (Desal G-10 and Desal G-20) through streaming potential measurements and the feed solution concentration (C_f), of the type of a Freundlich isotherm [Eq. (2)].

$$\ln C_M = a + b \ln C_f \quad (2)$$

The Desal G-20 membrane, the one bearing a higher surface charge, appeared to display a logarithmic relationship for NaCl [Eq. (3)]:

$$\ln C_M\,(\mathrm{mol/m^3}) = 3.57 + 0.475 \ln C_f\,(\mathrm{mol/m^3}) \quad (3)$$

Furthermore, the surface charge of Desal G-20 was likely to be partially due to the adsorption of anions from the solution onto the membrane surface. Wang et al. [103] concluded that NF45 membrane was expected to be suitable for the separation of the mixture solutions of bivalent anion electrolytes or neutral organic solutes with a few hundreds of MW and univalent anion electrolytes or neutral organic solutes with several 10-folds of MW. The experimental results indicated that the rejection of organic solutes and inorganic electrolytes by the NF45 membrane from high to low were ranked as:

$$\text{Raffinose} > Na_2SO_4 > MgSO_4 > \text{sucrose} > \text{glucose} >> KCl = NaCl > MgCl_2 > \text{glycerin}$$

Recently, Matsuura [113] provided several directions in which progress in separation can be improved in the future. For NF membranes, it was shown that improvement of productivity by higher flux membranes was achieved through the development of thin-film composites with a very thin selectivity skin layer. In addition, Kurihara et al. [114] attributes the higher productivity of current membranes to an increase in surface roughness. Other methods used to improve membrane performance including development of mixed-matrix membrane materials including hybrid organic-inorganic materials and the surface modification of membranes. These improvements are not only limited to higher flux at lower operating pressures but also in terms of less fouling propensity, higher chlorine tolerance and increased solvent resistance [115].

6. Modelling of NF membranes

A good predictive model will allow users to obtain membrane characteristics, predict process performance as well as optimize the process. The ability to develop such modelling techniques successfully will result in a smaller number of experiments and subsequently save time and money in the development stage of a process [116].

6.1. Models based on the extended Nernst-Planck equation

For NF membranes, the most commonly adapted models were those based on the extended Nernst-Plank equation [Eq. (4)]:

$$j_i = -D_{i,p}\frac{dc_i}{dx} - \frac{z_i c_i D_{i,p}}{RT} F \frac{d\Psi}{dx} + K_{i,c} c_i J_v \quad (4)$$

Tsuru et al. [117] first proposed such a model for NF membranes, describing the transport of ions in terms of an effective membrane thickness: porosity ratio (m) $\Delta x/A_k$, and an effective membrane charge density (mol.m^{-3}) X_d. The model was successful in describing the rejection of mixed salt solutions. In a later work [118], a similar model, but with the inclusion of steric effects, was used to model the transport of organic electrolytes in the presence of Na^+ and Cl^- ions.

The electrostatic and steric-hindrance (ES) model was developed from the steric-hindrance pore model and the Teorell-Meyer-Sievers model. The new model is used to predict the transport performance of charged solutes through NF membranes based on their charged pore structure: an aqueous solution of different tracer charged solutes (sodium benzenesulfonate, sodium naphthalenesulfonate and sodium tetraphenyl-borate) and a supporting salt (sodium chloride) to verify the ES model. The prediction based on the ES model was in good agreement with the experimental results.

Bowen and Mukhtar [119] suggested a hybrid model in rejection of a single electrolyte at six NF membranes. The hybrid model is based on the extended Nernst-Planck equation with a Donnan condition at the membrane/solution interfaces and the hindered nature of transport in the membranes. Such an interpretation allows a characterization of the membranes in terms of two parameters, effective membrane thickness (Δx) and effective membrane charge density (X). A knowledge of the effective membrane thickness, effective charge density and effective pore size allows use of the model to predict the separation of mixtures of electrolytes at a membrane. Very good agreement between such a prediction and experimental data has been obtained.

Bowen et al. [120] were the first to coin the term "Donnan-steric-pore model" (DSPM) that was a modified form of a hybrid model. The model takes into account the hindrance effects for diffusion and convections to allow for transport of ions/charged solutes taking place within a confined space inside the membranes. This inclusion allows the membrane to be characterized in terms of an effective pore radius, r_p, in addition to $\Delta x/A_k$ and X_d. Subsequent studies [121,122] showed that the model can predict the rejection performance very well of single salt solutions.

Recently, Bowen and Wellfoot [123] suggested modifications to the DSPM models for NF membranes. The first modification was used to take into account the effects of log-normal pore size distributions on the rejection of uncharged solutes and NaCl at hypothetical NF membranes. The results showed that the effect of pore-wise variation in viscosity is less apparent when considered at a defined applied pressure rather than at a defined flux, showing a further advantage of basing theoretical analysis of NF in terms of applied pressure. Truncated pore size distributions gave better agreement than full distributions with experimental rejection data the for NF membrane. The second modification was developed to calculate the uncharged solute rejection on the basis of a single membrane parameter (pore radius). The theoretical description is based on a hydrodynamic model of hindered solute transport in pores. The good agreement between this model and experimental data confirms that uncharged solute rejection in NF membranes may be well-described by such a continuum model.

The surface properties of membranes have been characterized in terms of potential in the Outer Helmholtz Plane (Ψd) [124]. A theoretical

analysis of electrical and electrokinetic phenomena (electrolyte conductivity inside pores λ_{pore}, membrane potential, E_m, and streaming potential (SP) occurring in charged capillaries was developed in the framework of the linear thermodynamics of irreversible processes with the aim of studying the variation of SP, E_m and λ_{pore} as a function of Ψd for various pore sizes and electrolyte concentrations. The analysis established the variation of λ_{pore}, E_m and SP vs. the Outer Helmholtz Plane potential (Ψd). On the other hand, a comprehensive semi-empirical mathematical model based on the Poisson–Boltzmann equation, membrane surface charge model, was developed [125] to investigate the effects of solution physico-chemistry on the zeta potential of NF membranes. The correlations between the zeta potential, surface charge density and solution chemistry were well delineated by this new model.

6.2. Models based on the Spiegler–Kedem model

Another approach for NF modeling is through the Spiegler–Kedem model [126–129]. This black-box approach allows the membranes to be characterized in terms of salt permeability, P_s, and the reflection coefficient σ. This model is in the first instance limited to binary salt systems, and in the limiting case to a binary salt system in the presence of a completely rejected organic ion [127,129].

A rejection of perchlorate anion (ClO_4^-) using NF and UF membranes was performed by Yoon et al. [130]. The data obtained were modelled by application of a non-equilibrium thermodynamic model. The model has five parameters: molecular transport coefficient (w), osmotic pressure gradient ($\Delta\Pi$), molecular reflection coefficient (σ), the average bulk fluid interfacial concentration between the feed and permeate side (C_{avg}), and the solvent flux (J_v). The results indicated that, in a pure component system, target ions (in this case ClO_4^-) can be excluded from (negatively) charged membranes with larger pores with respect to the size of the ion, but this rejection capability is quickly lost in the presence of a sufficient amount of other ions that can screen the apparent electrostatic force field. As intuitively expected, the perchlorate flux is governed by convection in large-pore membranes. Another model was developed by Pontalier et al. [131]; it describes mass transfer through the combination of convective–diffusive flux in the pores and diffusive flux in the membrane material. This model supposed solute transfer only occurs in the pores while solvent can also pass through the membrane material. Solute and solvent fluxes then depend on sieving effect, friction and electrostatic forces, permeability and pore radius of the membrane. All these characteristics were introduced in the model via five parameters which can be estimated from experimental data. This model could be used for the optimization of the NF process.

Diawara et al. (132) used an NF45 membrane to treat highly fluorinated brackish drinking water. Their approach was based on the phenomenological model of Spiegler, Kedem and Katchalsky (SKK) under dilute solution conditions but neglected the charges carried by the membrane. Experimental results showed for the first time that selective defluorination can occur using a NF membrane. The rejection was around 96%. The phenomenological parameters σ (the membrane reflection coefficient) and P_s (the solute permeability) were calculated, and it was observed that σ could be linked linearly to the hydration energy of the halide ions as shown in Eq. (5). Furthermore, P_s appeared to be linked to the type of electrolyte.

$$\sigma\ (\text{kJ/ mol}) = 0.01397 + 0.00212\ E_{hyd}\ (\text{kJ/mol}) \quad (5)$$

The SKK model was also used by Van der Bruggen and Vandecasteele [133] to develop a model for the retention of organic molecules with a given NF membrane at different pressures as a

function of the molecular weight. It was shown that for the UTC-20 membrane, a transmembrane pressure of 8–10 bar is optimal in view of the retentions. This is helpful in the choice of the operating pressure for practical applications, in addition to economical considerations such as energy requirements, working costs and investment costs.

6.3. Sophisticated modifications to the models

Hagmeyer and Gimbel [134] proposed to incorporate the change of the dielectric constant between bulk and pore solution to calculate the ion distribution between bulk and pore solution. Based on the extended Nernst-Planck equation, the developed model was used to model the data obtained from the rejection of single salt solutions at different concentrations, the rejection of ternary ion mixtures as well as the rejection at different pH values by NF membranes. The decrease of NaCl rejection as well as the increase of $CaCl_2$ rejection was well described by the model. The rejections of ternary ion mixtures of $NaCl/Na_2SO_4$ and $NaCl/CaCl_2$ were determined experimentally and were predicted by the model except for the $NaCl/CaCl_2$ mixture in a NF membrane where the negative rejections of Na^+ were observed but not predicted.

Lefebvre et al. [135] studied the rejection of single salts and a multi-electrolyte mixture experimentally and theoretically using a loose ceramic TiO_2 membrane over a certain range of operating conditions (pH and feed salt concentration). The results were compared with those obtained by an organic NF membrane (NF200). Theoretical ion rejection predictions for multi-electrolyte solutions are obtained by numerically solving the hindered transport extended Nernst-Planck (ENP) ion flux equations using the computer simulation program, NANOFLUX, which incorporates electrostatic, steric, and hydrodynamic interactions and a new choice for ion size (bare crystal, or Pauling, radius). The results showed that the looser ceramic nanofilter does not necessarily perform less well than the organic one. In all operating conditions, the rejection of Ca^{2+} is very high compared to the rejection of Na^+. This was due to the sign of a positive membrane charge. The high rejection of Ca^{2+} for positively charged membranes is mainly due to a strong Donnan/steric exclusion at the feed/membrane interface. The low rejection of Na^+ for positively charged membranes is due to its relatively weak Donnan/steric exclusion combined with its electrical migration in the streaming potential, which tends to favor the transmission of co-ions. The authors concluded that their method could lead to a cost-effective way for choosing appropriate NF membranes, optimizing the implementation of industrial NF processes, and finally dimensioning industrial-scale NF plants.

Based on the Maxwell–Stefan transport equations, Straatsma et al. [136] developed a NF membrane filtration model to calculate the permeate flux and rejections of multi-component liquid feeds as a function of membrane properties (mean pore size, porosity, thickness, surface charge characteristic) and feed pressure. A Freundlich equation was used to describe the membrane charge by means of adsorption of ions.

Recently Bandini and Vezzani [137] presented a general model called the Donnan steric pore model (DSPM) and dielectric exclusion model to describe mass transfer of electrolytes and neutral solutes through NF membranes. In this model, ionic partitioning at the interfaces between the membrane and the external phases takes into account three separation mechanisms: steric hindrance, Donnan equilibrium and dielectric exclusion. The membrane is characterized through the use of adjustable parameters such as average pore radius, effective membrane thickness and volumetric charge density. The separation effect related to the dielectric exclusion is relevant with respect to the Donnan equilibrium in determining bivalent counter-ion rejection, such as $CaCl_2$ as well as $MgSO_4$, whereas

dielectric effects are not so remarkable in the case of mixtures containing various co-ions, such as $NaCl + Na_2SO_4$.

van de Lisdonk et al. [138] presented a model, called the Supersaturation Prediction Model, which is able of calculating the supersaturation ratios of sparingly soluble compounds at the membrane surface. The model is a combination of a concentration polarization model and a model for calculation of the supersaturation ratio of sparingly soluble compounds, especially calcium carbonate and barium sulphate.

6.4. Incorporating concentration polarization effect

Concentration polarization (CP) is a serious problem that has restricted the use of membranes. Bhattacharjee et al. [139] developed a coupled model of CP and pore transport of multicomponent salt mixtures in crossflow NF. This model predicts local variations of ionic concentrations, flux and individual ion rejections along a rectangular crossflow filtration channel for three-component salt mixtures by a coupled solution of the convective-diffusion equation, which governs the transport of salt ions in the boundary layer adjacent to the membrane, and the extended Nernst-Planck equation, which governs the ion migration through the membrane pores. The two transport models are coupled through boundary conditions at the membrane feed–solution interface. The influence of a wide variety of fundamental physico-chemical parameters and operating conditions on the intrinsic and observed rejection were predicted by this model.

Bowen and Mohammad [140] and Mohammad [141] modified the DSPM model to take into account the CP effect for mixture of charged ions/solutes. With this approach, the permeate flux was calculated based on the concentration of ions/charged solutes at the membrane surface. The CP effect was taken into account by describing the transport of multi-component ions and solute in the mass transfer film layer using the extended Nernst-Planck equation. In such a manner, the permeate fluxes were predicted based on the osmotic pressure determined at the membrane interface. A comparison of the model calculation with published experimental data shows that the model can predict the pattern of rejection and flux reduction behavior quite well for systems containing NaCl-dye-H_2O.

de Pinho et al. [142] used computational fluid dynamics (CFD) for the modeling of NaCl transport occurring at the fluid phase adjacent to a NF membrane based on a diffusion and convection mechanism. The results gave a rigorous assessment of the CP and the determination of intrinsic rejection coefficients, f_{exp}, that are dependent on the membrane characteristics and on the operating conditions of the transmembrane pressure and feed solute concentration. In this work, experimental data of permeate solute concentrations and fluxes, generated by NF tests of solutions of neutral solutes, were used as boundary conditions in CFD. The strong effect of solute concentration due to membrane–ion electrostatic interactions was accounted for in the model through diffusion and convection hindrance factors that are concentration dependent. There is excellent agreement between predictions and experimental results.

Geraldes et al. [143] suggested a numerical model based on the finite volume formulation to predict laminar flows hydrodynamics and mass transfer of aqueous solutions in the feed channel of spiral-wound and plate-and-frame systems for NF membranes. This model was studied through an integrated approach using CFD for the modelling of the fluid phase with appropriate boundary conditions that took into account the solute transport inside the membrane. The authors analyzed the CP at the surface of the NF membrane by correlating concentration boundary layer thickness [Eq. (6)], which is based on the CFD predicted values of the solute concentration profiles:

$$\frac{\delta_\omega}{h} = 15.5\left(\frac{l}{h}\right)^{0.4} Re^{-0.4} Sc^{-0.63} Re_p^{-0.04} \left(1 - 186\, Sc^{-1.0} Re_p^{-0.21}\right) \quad (6)$$

This equation was valid in the operating condition ranges of $250 < Re < 1000$, $0.02 < Re_p < 0.1$ and $800 < Sc < 3200$. This correlation shows that higher circulation Reynolds numbers lead to a smaller CP. Additionally, for a given circulation Reynolds number, higher values of both the permeation Reynolds and Schmidt numbers induced an increase of the CP.

6.5. Models for economic assessment

There have been very few works on establishing an economic assessment model specifically for NF membranes. Sethi and Wiesner [144] developed a cost model to simulate the membrane systems. In this study, treatment costs and cost effectiveness of a hollow-fiber NF (HFNF) system vs. an integrated system comprised of spiral-wound NF (SWNF) pretreated with hollow-fiber UF (HFUF) were estimated and compared. It was concluded that for smaller facilities, single NF is preferable to treat raw water. At small plants the integrated HFUF–SWNF treatment train demonstrated higher non-membrane capital costs, which constitute the major component of total costs. However, when the raw water is largely characterized by particles with a very high fouling potential for the single HFNF step, separate HFUF pretreatment for particulate removal may be warranted. Operating the HFUF system at higher feed pressures, and consequently higher permeate fluxes, was predicted to improve the cost effectiveness of the integrated HFUF–SWNF system, particularly for raw waters characterized by larger particles.

Verberne et al. [145] established a model for cost estimation of a NF membrane system based on projected practical data and an actual tender from suppliers. The Verberne cost model was used by Bruggen et al. [17] to assess an economic aspect of treatment systems for the elimination of pesticides, nitrate and hardness from soil water.

7. Atomic force microscopy (AFM)

Atomic force microscopy (AFM) [146] gives topographic images by scanning a sharp tip over a surface. It has become an important means of imaging the surface of materials at up to atomic level resolution. The technique has therefore attracted the interest of a number of researchers interested in the surface properties of membranes [147].

The study of the surface morphology of membranes can help explain the separation processes in these membranes such as the characteristics of pore structure (pore diameter, pore density and pore size distribution) and to determine their filtration properties [148]. An atomic force microscope may be used in a number of different modes in air and even in liquids. The most widely used is the "contact mode" in which the tip responds to a very short range of repulsive (Born) forces. A second mode of operation is the "non-contact mode" in which the tip responds to attractive van-der-Waals interactions with the sample [147].

Contact atomic force and scanning tunneling microscopes have been used by Bessieres et al [149] to investigate the surface of polymeric UF and MF membranes. Experiments were performed in air and in a liquid environment. The microscopic techniques discerned pore diameters in the range of 11 to 114 nm for 40 to 200 kDa MWCO SPS UF membranes and confirmed a mean pore diameter of 96 nm for the 0.1/zm PVDF MF membrane. AFM and scanning electron microscopy (SEM) were used to investigate the surface structure and topography of polyvinylidene fluoride MF membranes [150]. AFM

reveals very uniform nodule aggregates with intermediate sized pores in their interstitial regions.

Non-contact AFM has been used by many researchers. Bowen et al. [151] used non-contact AFM to investigate the surface pore structure of eight Diaflo UF membranes covering a range of nominal MWCO from 3000 to 300,000. These membranes were manufactured from three different polymer types. Analysis of the pore images gave quantitative information on the surface pore structure, in particular the pore size distribution and surface roughness. Another study using non-contact AFM was conducted by Bowen et al [152] for a UF membrane with a 25,000 MWCO. Analysis of the images gave a mean pore size of 5.1 nm with a standard deviation of 1.1 nm.

On the other hand, AFM was used to scan the surface pore structure of cyclopore and anopore MF membranes in air [148]. This work showed that non-contact AFM is able to image the original surface of MF membranes in air with single pore resolution. Analysis of the images gave quantitative information on the surface pore structure, in particular the pore size distribution. Non-contact AFM was used also by Calvo et al. [153] to determine pore size distributions, internal surface area and size of surface pores for two polyether sulphonic microporous composite membranes with nominal MWCOs of 4000 and 30,000 Da. The results were compared by N_2 adsorption–desorption at 77 K and a liquid displacement technique.

Fritzche et al. [154] used contact and non-contact AFM and SEM to investigate the surface structure and morphology of 30 kDa membranes from different materials. The surface was found to have a network like fine structure. Their results indicated pores with diameters in the 12–20 nm range. Bottino et al. [155] used AFM to study the surface of UF and MF ceramic membranes. They showed that AFM can provide information on both size and shape of Al_2O_3 particles constituting the selective skin layer as well as the surface roughness of the skin. For MF membranes, they reported similar results to those obtained by conventional SEM.

Later, AFM was used to show the fouling behavior of cellulose acetate and aromatic polyamide thin-film composite RO membranes [156]. First, the laboratory-scale colloidal fouling tests were used to compare the fouling behavior between two membranes. Results showed a significantly higher fouling rate for the thin-film composite membranes compared to the cellulose acetate membranes. The higher fouling rate was attributed to surface roughness which is inherent in interfacially polymerized aromatic polyamide composite membranes. AFM and SEM images of the two membrane surfaces strongly support this conclusion. These surface images reveal that the thin-film composite membrane exhibits large-scale surface roughness of a ridge-and-valley structure, while the cellulose acetate membrane surface is relatively smooth.

AFM was used for the first time to quantify directly the adhesive force between a colloid probe and two polymeric UF membranes of similar MWCO (4000 Da) but different materials [ES 404 and XP 117, PCI Membrane Systems (UK)] [157]. It was found that the adhesive force at the ES 404 membrane was more than five times greater than that at the XP 117 membrane. The development of such a sensor (colloid probe) for quantifying the adhesive force at membrane surfaces allowed a relatively fast procedure for assessing the potential fouling of membrane surfaces by particles. This should facilitate the development of new membrane materials with low or zero fouling properties.

The geometry of AFM cantilever tips is not simple, and in some cases not precisely known, making comparison with theory difficult. However, attaching a sphere to the cantilever instead of a tip makes it possible to measure interactions between surfaces of known geometry and hence facilitates theoretical interpretation of the results [158]. Such attached spheres are termed colloid

probes. Thus, Hilal and Bowen [159] used AFM in conjunction with the colloid probe technique to study the electrical double layer interactions between a 0.75 μm silica sphere and a polymeric microfiltration track etch cyclopore membrane (nominally 1 μm) in aqueous solutions. The silica colloid probe was used to image the membrane surface (using the double layer mode) at different imaging forces in high purity water and at a constant imaging force in sodium chloride solutions of different ionic strengths at pH 8. The results provided experimental evidence on the influence of electrostatic double layer interactions on the rejection at the pores of a MF membrane. The electrostatic repulsive force as a single colloid approaches a membrane was directly measured, and scanning of the membrane surface with the colloid probe provided direct visualisation of the membrane surface as it would be experienced by the a colloidal particle during flirtation.

Another study of adhesive force between both the protein bovine serum albumin and a yeast cell at two different membranes was conducted by Bowen et al. [160]. These were polymeric UF membranes of similar MWCO (4000 Da) but of different materials (ES 404 and XP 117, PCI Membrane Systems, UK). It was found that for both protein and cell systems that the adhesive force at the ES 404 membrane was greater than that at the XP 117 membrane.

Bowen et al. [120] also used AFM to characterize a NF membrane (Hoechst, PES5). AFM allows direct determination of surface pore radius and surface porosity. The AFM images provided direct confirmation of the presence of discrete surface pores in such membranes. The first AFM comparative study of NF membranes was considered by Bowen et al. [161]. Surface morphology, pore size distribution and particle adhesion of three NF membranes were quantified by AFM. The NF membranes used were AFC30, AFC80 and XDA9920 from PCI. The AFC series was thin-film composite membranes that were

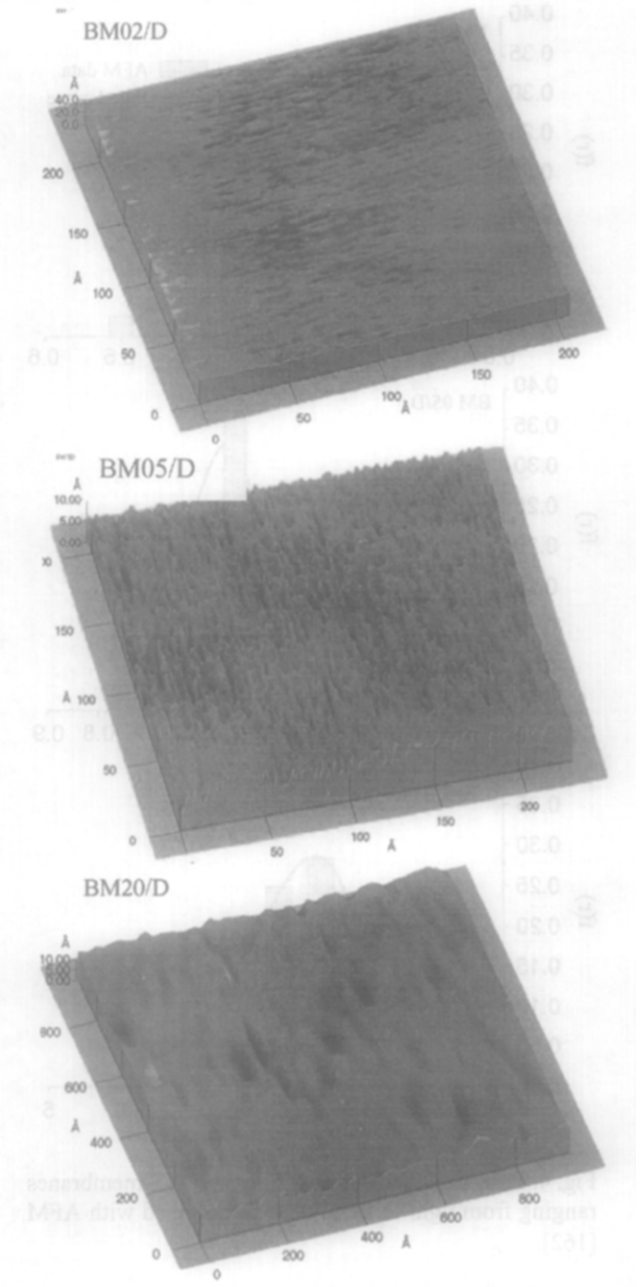

Fig. 3. AFM images of three NF membranes ranging from tight to very loose [162].

negatively charged, while the XDA9920 was manufactured from a positively charged polymer blend. The results showed that the mean pore

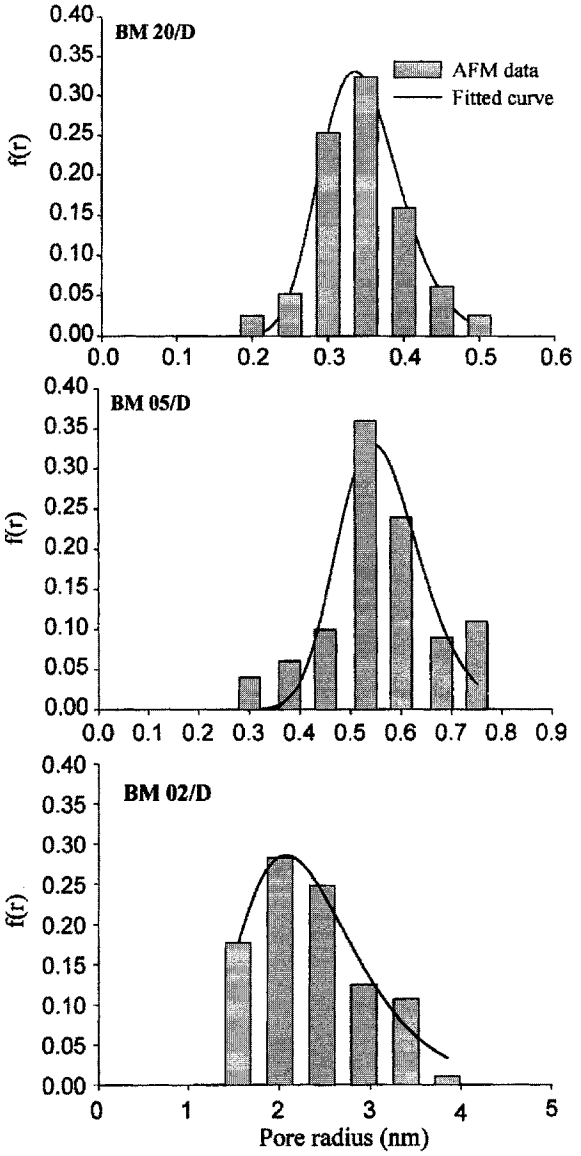

Fig. 4. Pore size distribution of the three NF membranes ranging from tight to very loose as obtained with AFM [162].

diameters were ~1 nm. Use of the colloid probe technique allowed quantification of the adhesion of polystyrene and silica particles to the membrane surfaces. Adhesion of polystyrene particles was greater than that of silica particles, due partly to a greater electrostatic double-layer repulsion between the negatively charged membrane and silica, and partly to a short-range repulsive interaction associated with the silica surface.

In a recent work, Mohammad et al. [162] used AFM to image three NF membranes ranging from very tight (200 MWCO), loose (500 MWCO) and very loose (2000 MWCO) membranes. Fig. 3 shows the images of the membranes, while Fig. 4 shows the pore size distribution obtained using the AFM measurements. A comparison with data obtained from solute rejection studies showed that the average pore size obtained through AFM was relatively acceptable. It can be seen that AFM is a very useful tool for surface morphology studies of NF membranes albeit for very tight, low-MWCO membrane properties.

In another work, Mohammad et al. [163] produced NF membranes with varying properties through an interfacial polymerization technique. AFM was again used as one of the tools to determine the variation in the membrane properties. The properties include pore size, effective charge density and effective membrane thickness. The results showed that increasing the reaction time resulted in decreasing water permeabilities, but based on AFM imaging, the pore size was of similar value. Increasing the monomer concentration resulted in decreasing water permeabilities. However, based on AFM imaging the pore size differed considerably.

8. Conclusions

A comprehensive review is given of (1) the use of NF membranes in water and wastewater treatment, (2) NF membrane fouling, (3) the mechanisms of separation, (4) NF modelling, and (5) use of AFM. It was shown that NF membranes can be used to treat water by removing contaminants and organics such as natural organic matter, disinfection by-product, pesticides, dissolved uranium, arsenite, chromate, and other metals. In addition, NF was used as a pretreat-

ment in the desalination process to prevent SWRO membrane fouling, prevent scaling (both in SWRO and MSF) and lower the required pressure to operate SWRO plants.

Fouling problems will lead to higher operation costs: higher energy demand, increase of cleaning and reduced life time of the membrane elements. The separation mechanism of NF has been identified mostly due to charge and steric effects. A large majority of modeling works on NF has been by models based on the extended Nernst-Planck equation. A good model will lead towards better prediction and optimization of NF membrane processes.

Finally, state-of-the-art AFM has been mentioned in this review, which can significantly characterize the surface of NF membranes. Surface morphology, pore size distribution and particle adhesion of NF membrane were able to be quantified by AFM.

9. Symbols

c — Concentration in membranes, mol/m^3
C_f — Feed solution concentration, mol/m^3
C_M — Effective surface charge, mol/m^3
d — Membrane cut-off (Dalton)
D — Diffusion coefficient, m^2/s
$D_{i,p}$ — Hindered diffusivity, m^2/s
E_{hyd} — Hydration energy, kJ/mol
F — Faraday constant, C/mol
h — Channel height, m
I — Ion strength, mM
J — Membrane flux, LMH
J_0 — Initial flux, LMH
j_i — In flux (based on membrane area), mol/m^{2}s^{-1}
$K_{i,c}$ — Hindrance factor for convection
J_v — Volume flux (based on membrane area), m/s
l — Channel length, m
P — Operating pressure, psi
t — Time, s
R — Gas constant, J/mol K
Re — Circulation Reynolds number defined by $Re = \rho u 0 h/\mu$
Re_p — Permeation Reynolds number defined by $Re_p = \rho v p h/\mu$
Sc — Schmidt number
T — Temperature, K
x — Distance normal to membrane, m
z_i — Valence of ion

Greek

σ — Reflection coefficient, kJ/mol
Ψ — Electric potential, V
δ_ω — Boundary layer thickness

Acknowledgements

We thank The Middle East Desalination Research Centre (MEDRC) for funding this work.

References

[1] X. Lu, X. Bian and L. Shi, Preparation and characterization of NF composite membrane, J. Membr. Sci., 210 (2002) 3–11.
[2] B.Van der Bruggen and C. Vandecasteele, Removal of pollutants from surface water and groundwater by nanofiltration: overview of possible applications in the drinking water industry, Environ. Poll., 122 (2003) 435–445.
[3] W.J., Conlon and S.A McClellan, Membrane softening: treatment process comes of age, J. AWWA, 81 (1989) 47–51.
[4] J. Schaep, B. Van der Bruggen, S. Uytterhoeven, R. Croux, C. Vandecasteele, D. Wilms, E. Van Houtte and F. Vanlerberghe, Removal of hardness from groundwater by nanofiltration, Desalination, 119 (1998) 295–302.
[5] H.D.M Sombekke, D.K. Voorhoeve and P. Hiemstra, Environmental impact assessment of groundwater treatment with nanofiltration, Desalination, 113 (1997) 293–296.

[6] R.A Bergman, Membrane softening versus lime softening in Florida—a cost comparison update, Desalination, 102 (1995) 11–24.
[7] R.A. Bergman, Cost of membrane softening in Florida, J. AWWA, 88 (1996) 32–43.
[8] B.M Watson and C.D. Hornburg, Low-energy membrane nanofiltration for removal of color, organics and hardness from drinking-water supplies, Desalination, 72 (1989) 11–22.
[9] P. Fu, H. Ruiz, K. Thompson and C. Spangenberg, Selecting membranes for removing NOM and DBP precursors, J. AWWA, 86 (1994) 55–72.
[10] P. Fu, H. Ruiz, J. Lozier, K. Thompson and C. Spangenberg, A pilot study on groundwater natural organics removal by low-pressure membranes, Desalination, 102 (1995) 47–56.
[11] J.G. Jacangelo, R.R. Trussell and M. Watson, Role of membrane technology in drinking water treatment in the United States, Desalination, 113 (1997) 119–127.
[12] I.C. Escobar, S. Hong and A. Randall, Removal of assimilable and biodegradable dissolved organic carbon by reverse osmosis and nanofiltration membranes, J. Membr. Sci., 175 (2000) 1–17.
[13] W.R. Everest and S.A. Malloy, Design/build approach to deep aquifer membrane treatment in Southern California, Desalination, 132 (2000) 41–45.
[14] A. Khalik and V.S. Praptowidodo, Nanofiltration for drinking water production from deep well water, Desalination, 132 (2000) 287–292.
[15] M. Alborzfar, K. Escande and S.J. Allen, Removal of natural organic matter from two types of humic ground waters by nanofiltration, Water Res., 32 (1998) 2970–2983.
[16] A. Gorenflo, D. Veliizquez-Padrh and F.H. Frimmel, Nanofiltration of a German groundwater of high hardness and NOM content: performance and costs, Desalination, 151 (2002) 253–265.
[17] B. Van der Bruggen, J. Schaep, W, Maes, D. Wilms and C. Vandecasteele, Nanofiltration as a treatment method for the removal of pesticides from ground waters, Desalination, 117 (1998) 139–147.
[18] B. Van der Bruggen, K. Everaert, D. Wilms and C. Vandecasteele, The use of nanofiltration for the removal of pesticides from ground water: an evaluation, Water Sci. Technol.: Water Supply, 1 (2001) 99–106.
[19] B. Van der Bruggen, K. Everaert, D. Wilms and C. Vandecasteele, Application of nanofiltration for the removal of pesticides, nitrate and hardness from ground water: retention properties and economic evaluation, J. Membr. Sci., 193 (2001) 239–248.
[20] E. Wittmann, P. Cote, C. Medici, J. Leech and A.G. Turner, Treatment of a hard borehole water containing low levels of pesticide by nanofiltration, Desalination, 119 (1998) 347–352.
[21] Y. Kiso, Y. Nishimura, T. Kitao and K. Nishimura, Rejection properties of non-phenylic pesticides with nanofiltration membranes. J. Membr. Sci., 171 (2000) 229–237.
[22] Y. Kiso, A. Mizuno, R. Binti Othman, Y. Jung, A. Kumanoc and A. Arijic, Rejection properties of pesticides with a hollow fiber NF membrane (HNF-1), Desalination, 143 (2002) 147–157.
[23] P. Berg, G. Hagmeyer and R. Gimbel, Removal of pesticides and other micropollutants by nanofiltration, Desalination, 113 (1997) 205–208.
[24] T. Montovay, M. Assenmacher and F.H. Frimmel, Elimination of pesticides from aqueous solution by nanofiltration, Magyar Kemiai Folyoirat,102 (1996) 241–247.
[25] G. Ducom and C. Cabassud, Interests and limitations of nanofiltration for the removal of volatile organic compounds in drinking water production, Desalination, 124 (1999) 115–123.
[26] R. Kettunen and P. Keskitalo, Combination of membrane technology and limestone filtration to control drinking water quality, Desalination, 131 (2000) 271–283.
[27] A.G. Pervov, E.V. Dudkin, O.A. Sidorenko, V.V. Antipov, S.A. Khakhanov and R.I. Makarov, RO and NF membrane systems for drinking water production and their maintenance techniques. Desalination, 132 (2000) 315–321.
[28] O. Raff and R.D. Wilken, Removal of dissolved uranium by nanofiltration, Desalination, 122 (1999) 147–150.
[29] T. Urase, J. Oh and K. Yamamoto, Effect of pH on rejection of different species of arsenic by nanofiltration, Desalination, 117 (1998) 11–18.
[30] H. Yeh, I. Tseng, S. Kao, W. Lai, J. Chen, G. Wang and S. Lin, Comparison of the finished water quality among an integrated membrane process, conventional and other advanced treatment processes,

Desalination, 131 (2000) 237–244.
[31] B. Levine, K. Madireddi, V. Lazarova, M. Stentrom and M. Suffet, Treatment of trace organic compounds by membrane processes: at the Lake Arrowhead water reuse pilot plant, Water Sci. Technol., 40(4-5) (1999) 293–301.
[32] C. Visvanathan, B. Marsono and B. Basu, Removal of THMP by nanofiltration: effects of interference parameters, Water Res., 32(12) (1998) 3527–3538.
[33] K.M. Agbekodo, B. Legube and P. Cote, Organics in NF permeate, J. AWWA, 88(5) (1996) 67–74.
[34] J.W. Cho, G. Amy and J. Pellegrino, Membrane filtration of natural organic matter: initial comparison of rejection and flux decline characteristics with ultrafiltration and nanofiltration membranes, Water Res., 33(11) (1999) 2517–2526.
[35] B. Ericsson, M. Hallberg and J. Wachenfeldt, Nanofiltration of highly colored raw water for drinking water production, Desalination, 108 (1996) 129–141.
[36] M. Thanuttamavong, K. Yamamotob, J. Oh, K. Chood and S. Choi, Rejection characteristics of organic and inorganic pollutants by ultra low-pressure nanofiltration of surface water for drinking water treatment, Desalination, 145 (2002) 257–264.
[37] I. Koyuncu and M. Yazgan, Application of nanofiltration and reverse osmosis membranes to the salty and polluted surface water, J. Environ. Sci. Health, A36(7) (2001) 1321–1333.
[38] P. Laurent, P. Servais, D. Gatel, G. Randon, P. Bonne and J. Cavard, Microbiological quality before and after nanofiltration, J. AWWA, 91(10) (1999) 62–72.
[39] M.T. Yahya, C.B. Blu and C.P. Gerba, Virus removal by slow sand filtration and nanofiltration, Water Sci. Technol., 27(3–4) (1993) 445–448.
[40] M. Otaki, K. Yano and S. Ohgaki, Virus removal in a membrane separation process, Water Sci. Technol., 37(10) (1998) 107–116.
[41] T. Urase, K. Yamamoto and S. Ohgaki, Effect of pore structure of membranes and module configuration on virus retention, J. Membr. Sci., 115(1) (1996) 21–29.
[42] C Reiss, J. Taylor and C. Robert, Surface water treatment using nanofiltration — pilot testing results and design considerations, Desalination, 125 (1999) 97–112.
[43] J. De Witte, Surface water potabilisation by means of a novel nanofiltration element, Desalination, 108 (1997) 153–157.
[44] C. Ventresque and G. Bablon, The integrated nanofiltration system of the Méry-sur-Oise surface treatment plant (37 mgd), Desalination, 113 (1997) 263–266.
[45] J. Waypa, M. Elimelech and J. Hering, Arsenic removal by RO and NF membranes, J. AWWA, 89(10) (1997) 102–114.
[46] A. Seidel, J. Waypa and M. Elimech, Role of charge (Donnan) exclusion in removal of arsenic from water by a negatively charged porous nanofiltration membrane, Environ. Eng. Sci., 18(2) (2001) 105–113.
[47] E. Vroenhoek and J. Waypa, Arsenic removal from drinking water by a "loose" nanofiltration membrane, Desalination, 130 (2000) 265–277.
[48] P. Brandhuber and G. Amy, Alternative methods for membrane filtration of arsenic from drinking water, Desalination,117 (1998) 1–10.
[49] Y. Kiso, K. Takuji, K. Takane and N. Kazuyuki, Rejection properties of alkyl phthalates with nanofiltration membranes, J. Membr. Sci., 182 (2001) 205–214.
[50] S. Lee and R. Lueptow, Membrane rejection of nitrogen compounds. Environ. Sci. Technol., 35 (2001) 3008–3018.
[51] C. Ratanatamskul, Description of behavior in rejection of pollutants in ultra low pressure nanofiltration, Water Sci Technol., 38 (1998) 453–462.
[52] J. Redondo and F. Lanari, Membrane selection and design considerations for meeting European potable water requirements based on different feedwater conditions, Desalination, 113 (1997) 309–323.
[53] R. Molinari, P. Argurio and L.O. Romeo, Studies on interactions between membranes (RO and NF) and pollutants (SiO2, NO^{3-}, Mn^{++} and humic acid) in water, Desalination, 138 (2001) 271–281.
[54] B. Andrew, Sulphate removal by nanofiltration, Filtr. Sep., 38 (2001) 18–20.
[55] M. Afonso and R Yafiez, Nanofiltration of wastewater from the fishmeal industry, Desalination, 139 (2001) 429.
[56] R. Rautenbach and Th. Linn, High pressure reverse osmosis and nanofiltration, a "zero discharge" process combination for the treatment of waste water with severe fouling/scaling potential, Desalination, 105 (1996) 63–70.

[57] R. Rautenbach, T. Linn and L. Eilers, Treatment of severely contaminated waste water by a combination of RO, high-pressure RO and NF —potential and limits of the process, J. Membr. Sci., 174 (2000) 231–241.
[58] V. Geraldes and M. de Pinho, Process water recovery from pulp bleaching effluents by an NF/ED hybrid process, J. Membr. Sci., 102 (1995) 209–221.
[59] B. Schlichter, V. Mavrov and H. Chmiel, Study of a hybrid process combination ozonation and membrane filtration — filtration of model solution, Desalination, 156 (2003) 257–265.
[60] A. Hafiarle, D. Lemordant and M. Dhahbi, Removal of hexavalent chromium by nanofiltration, Desalination, 13 (2000) 305–312.
[61] I. Koyuncu, An advanced treatment of high-strength opium alkaloid processing industry wastewaters with membrane technology: pretreatment, fouling and retention characteristics of membranes, Desalination, 155 (2003) 265–275.
[62] A. Tang and V. Chen, Nanofiltration of textile wastewater for water reuse, Desalination, 143 (2002) 11–20.
[63] A. Bes-Pia, J. Mendoza-Roca, L. Roig-Alcover, A. Iborra-Clar, M. Iborra-Clar and M. Alcaina-Miranda, Comparsion between nanofiltration and ozonation of biologically treated textile waste water for it reuse in the industry, Desalination, 157 (2003) 81–86.
[64] I. Voigt, M. Stahn, St. Wohner, A. Junghans, J. Rost and W. Voigt, Integrated cleaning of coloured waste water by ceramic NF membranes, Sep. Purifi. Technol., 25 (2001) 509–512.
[65] R. Webar, H. Chmiel and V. Mavrov, Characteristics and application of new ceramic nanofiltration membrane, Desalination, 157 (2003) 113–125.
[66] D. Jakobs and G. Baumgarten, Nanofiltration of nitric acidic solutions from picture tube production, Desalination, 145 (2002) 65–68.
[67] M. Gonzilez, R. Navarro, I. Saucedo, M. Avila, J. Revilla and Ch. Bouchar, Purification of phosphoric acid solutions by reverse osmosis and nanofiltration, Desalination, 147 (2002) 315–320.
[68] B. Van der Bruggen and C. Vandecasteele, Distillation vs. membrane filtration: overview of process evolutions in seawater desalination, Desalination, 143 (2002) 207–218.
[69] J. Sikora, C. Hansson and B. Ericsson, Pre-treatment and desalination of mine drainage water in a pilot plant, Desalination, 75 (1989) 363–373.
[70] M. Al-Ahmad and F. Adbul Aleem, Scale formation and fouling problems effect on the performance of MSF and RO desalination,plants in Saudi Arabia, Desalination, 93 (1993) 287–310.
[71] S van Hoop, J.G. Minnery and B. Mack, Dead-end ultrafiltration as alternative pre–treatment to reverse osmosis in seawater desalination: a case study, Desalination, 139 (2001) 161–168.
[72] J. Redondo, Brackish-, sea- and wastewater desalination, Desalination, 138 (2001) 29–40.
[73] S. Bou-Hamad, M. Abdel-Jawad, S. Ebrahim, M. Al-Mansour and A. Al-Hijji, Performance evaluation of three different pretreatment systems for seawater reverse osmosis technique, Desalination, 110 (1997) 85–92.
[74] S. van Hoop, A. Hashim and A. Kordes, The effect of ultrafiltration as pretreatment to reverse osmosis in wastewater reuse and seawater desalination applications, Desalination, 124 (1999) 231–242.
[75] A. Brehant, V. Bonnelyeb and M. Perez, Comparison of MF/UF pretreatment with conventiotial filtration prior to RO membranes for surface seawater desalination, Desalination, 144 (2002) 353–360.
[76] C.K. Teng, M. Hawlader and A. Malek, An experiment with different pretreatment methods, Desalination, 156 (2003) 51–58.
[77] D. Vial and G. Doussau, The use of microfiltration membranes for seawater pre-treatment prior to reverse osmosis membranes, Desalination, 153 (2002) 141–147.
[78] D. Vial, G. Doussau and R. Galindo, Comparison of three pilot studies using Microza membrane for Mediterranean seawater pre-treatment, Desalination, 156 (2003) 43–50.
[79] A. Pervov, A. Andrianov, R.V. Efremov, A. Desyatov and A.E. Baranov, A new solution for Caspian seawater desalination: low pressure membrane, Desalination, 157 (2003) 377–384.
[80] A. Hassan, M. Al-So, A. Al-Amoudi, A. Jamaluddin, A. Farooque, A. Rowaili, A. Dalvi, N. Kither, G. Mustafa and I. Al-Tisan, A new approach to thermal seawater desalination processes using nanofiltration membranes (Part 1), Desalination, 118 (1998) 35–51.

[81] M. Al-Sofi , A. Hassan, G. Mustafa, A. Dalvi and M. Kither, Nanofiltration as a means of achieving higher TBT of ≥ 120 degrees C in MSF, Desalination, 118 (1998) 123–129.
[82] M. Al-Sofi, Seawater desalination — SWCC experience and vision, Desalination, 135 (2001) 121–139.
[83] A.M. Hassan, A. Farooque, A. Jamaluddin, A. Al-Amoudi, M. Al-Sofi, A. Al-Rubaian, N. Kither, I. Al-Tisan and A. Rowaili, A demonstration plant based on the new NF–SWRO process, Desalination, 131 (2000) 157–171.
[84] A. Criscuoli and E. Drioli, Energetic and exergetic analysis of an integrated membrane desalination system, Desalination, 124 (1999) 243–249.
[85] M. Mohesn, J. Jaber and M. Afonso, Desalination of brackish water by nanofiltration and reverse osmosis, Desalination, 157 (2003) 167.
[86] M. Potie, C. Diawara, M. Rumeau, D. Aureau and P. Hemmerey, Seawater nanofiltration (NF): fiction or reality? Desalination, 158 (2003) 277–280.
[87] E. Drioli, F. Laganh, A. Crlscuoh and G. Barbieri, Integrated membrane operations in desalination processes, Desalination, 122 (1999) 141–145.
[88] H. Ohya, T. Suzuki and S. Nakao, Integrated system for complete usage of components in seawater: A proposal of inorganic chemical combination seawater, Desalination, 134 (2001) 29–36.
[89] E. Drioli, A. Criscuoli and E. Curcioa, Integrated membrane operations for seawater desalination, Desalination, 147 (2002) 77–81.
[90] C. Visvanathafl, N. Boonthanon, A. Sathasivan and V. Jegatheesanb, Pretreatment of seawater for biodegradable organic content removal using membrane bioreactor, Desalination, 153 (2002) 133–140.
[91] M. Turek and P. Dydo, Hybrid membrane — thermal versus simple membrane system, Desalination, 157 (2003) 51–56.
[92] B. Van der Bruggen, L. Braeken and C. Vandecasteele, Evaluation, of parameters describing flux decline in nanofiltration of aqueous solutions containing organic compounds, Desalination, 147 (2002) 281–288.
[93] H. Vrouwenvelder, J. van Paassen, H. Folmer, A. Hofman Jan, M. Nederlof and D. Kooij, Biofouling of membranes for drinking water production, Desalination, 118 (1998) 157–166.
[94] A.I. Schafer, A.G. Fane and T. Waite, Fouling effects on rejection in the membrane filtration of natural waters, Desalination, 131 (2000) 215.
[95] J. Vrouwenvelder, J. Kappelhof, S. Heijman, J. Schippers and D. Kooij, Tools for fouling diagnosis of NF and RO membranes and assessment of the fouling potential of feed water, Desalination, 157 (2003) 361–365.
[96] S. Boerlage, M. Kennedy, A. Bonne Paul, G. Galjaard and J. Schippers, Prediction of flux decline in membrane systems due to particulate fouling, Desalination, 113 (1997) 231–233.
[97] J. Baker, T. Stephenson, S. Dard and P. Cote, Characterization of fouling of membrane used to treat surface water, Environ. Technol., 16 (1995) 977–985.
[98] J. Vrouwenvelder and D. Kooij, Diagnosis of fouling problems of NF and RO membrane installations by a quick scan, Desalination, 153 (2002) 121–124.
[99] A.I. Schafer, A.G Fane and T.D. Waite, Nanofiltration of natural organic matter: Removal, fouling and the influence of multivalent ions, Desalination, 118 (1998) 109–122.
[100] S. Hong and M. Elimelech, Chemical and physical aspects of natural organic matter (NOM) fouling of nanofiltration membranes, J. Membr. Sci., 132 (1997) 159–181.
[101] K. Kosutic and B. Kunst, RO and NF membrane fouling and cleaning and pore size distribution variations, Desalination, 150 (2002) 113–120.
[102] H. Shaalan, Development of fouling control strategies pertinent to nanofiltration membranes, Desalination, 153 (2002) 125–131.
[103] X. Wang, C. Zhang and P. Ouyang, The possibility of separating saccharides from a NaCl solution by using nanofiltration in diafiltration mode, J. Membr. Sci., 204 (2002) 271–28.
[104] K. Kosutic and B. Kunst, Removal of organics from aqueous solutions by commercial RO and NF membranes of characterized porosities, Desalination, 142 (2002) 47–56.
[105] B. Van der Bruggen, J. Schaep, D. Wilms and C. Vandecasteele, Influence of molecular size, polarity and charge on the retention of organic molecules by nanofiltration, J. Membr. Sci., 156 (1999) 29–41.

[106] S. Chellam and J. Taylor, Simplified analysis of contaminant rejection during ground- and surface water nanofiltration under the information collection rule, Water Res., 35 (2001) 2460–2474.
[107] J. Schaep, B. Van der Bruggen, C. Vandecasteele and D. Wilms, Influence of ion size and charge in nanofiltration, Separ. Purif. Technol., 14 (1998) 155–162.
[108] A. Lhassani, M. Rumeau, D. Benjelloun and M. Pontie, Selective demineralisation of water by nanofiltration application to the defluorination of brackish water, Water Res., 35 (2001) 3260–3264.
[109] J. Schaep and C. Vandecasteele, Evaluating the charge of nanofiltration membranes, J. Membr. Sci., 188 (2001) 129–136.
[110] J. Gilron, N. Gara and O. Kedem, Experimental analysis of negative salt rejection in nanofiltration membranes, J. Membr. Sci., 185 (2001) 223–236.
[111] J. Tanninen and M. Nystrom, Separation of ions in acidic conditions using NF, Desalination, 147 (2002) 295–299.
[112] M. Afonso, G. Hagmeyer and R Gimbel, Streaming potential measurements to assess the variation of nanofiltration membranes surface charge with the concentration of salt solutions, Separ. Purif. Technol., 22–23 (2001) 529–541.
[113] T. Matsuura, Progress in membrane science and technology for seawater desalination a review, Desalination, 134 (2001) 47–54.
[114] M. Kurihara and Y. Fusaoka, Maku [Membrane], 24 (1999) 247.
[115] S. Nunes and K. Peinemann, in: Membrane Technology in the Chemical Industry, S.P. Nunes and K.V. Peinemann, eds.,Wiley, Germany, 2001, pp. 1–53.
[116] N. Hilal, A.W. Mohammad, B. Atkin and N. Darwish, Using atomic force microscopy towards improvement in nanofiltration membrane properties for desalination pretreatment: a review, Desalination, 157 (2003) 137–144.
[117] T. Tsuru, S. Nakao and S. Kimura, Calculation of ion rejection by extended Nernst–Planck equation with charged reverse osmosis membranes for single and mixed electrolyte solutions, J. Chem. Eng. Japan, 24 (1991) 511–517.
[118] X.L. Wang, T. Tsuru, S. Nakao and S. Kimura, The electrostatic and steric–hindrance model for the transport of charged solutes through nanofiltration membranes, J. Membr. Sci., 135 (1997) 19–32.
[119] W. R. Bowen and H. Mukhtar, Characterisation and prediction of separation performance of nanofiltration membranes, J. Membr. Sci., 112 (1996) 263–274.
[120] W.R. Bowen, A. Mohammad and N. Hilal, Characterisation of nanofiltration membranes for predictive purposes use of salts, uncharged solutes and atomic force microscopy, J. Membr. Sci., 126 (1997) 91–105.
[121] J. Schaep, C. Vandecasteele, A.W. Mohammad and W.R. Bowen, Evaluation of the salt retention of nanofiltration membranes using the Donnan and steric partitioning model, Separ. Sci. Technol., 34(15) (1999) 3009–3030.
[122] J. Schaep, C. Vandecasteele, A.W. Mohammad and W.R. Bowen, Modelling the retention of ionic components for different nanofiltration membranes, Separ. Purif. Technol., 22–23(1–3) (2001) 169–179.
[123] W. Bowen and J. Welfoot, Modelling of membrane nanofiltration — pore size distribution effects, Chem. Engin. Sci., 57 (2002) 1393–1407.
[124] P. Fievet, A. Szymczyk, B. Aoubiza and J. Pagetti, Evaluation of three methods for the characterisation of the membrane–solution interface: streaming potential, membrane potential and electrolyte conductivity inside pores, J. Membr. Sci., 168 (2000) 87–100.
[125] J. Tay, J. Liu and D.D. Sun, Effect of solution physico-chemistry on the charge property of nanofiltration membranes, Water Res., 36 (2002) 585–598.
[126] P. Schirg and F. Widmer, Characterisation of nanofiltration membranes for the separation of aqueous dye-salt solutions, Desalination, 89 (1992) 89.
[127] R. Levenstein, D. Hasson and R. Semiat, Utilisation of the Donnan effect for improving electrolyte separation with nanofiltration membranes, J. Membr. Sci., 116 (1996) 77–92.
[128] X. Xu and H.G. Spencer, Dye-salt separations by nanofiltration using weak acid polyelectrolyte membranes, Desalination, 114 (1997) 129–137.
[129] M. Perry and C. Linder, Intermediate RO UF membranes for concentrating and desalting of low molecular weight organic solutes, Desalination, 71

(1989) 233.
[130] Y. Yoon, G. Amy, J. Chob, N. Her and J. Pellegrino, Transport of perchlorate (C104-) through NF and UF membranes, Desalination, 147 (2002) 11–17.
[131] P. Pontalier, A. Ismail and M. Ghoul, Specific model for nanofiltration, J. Food Engin., 40 (1999) 145–151.
[132] C.K. Diawara, S.M. Lo, M. Rumeau, M. Pontie and O. Sarr, A phenomenological mass transfer approach in nanofiltration of halide ions for a selective defluorination of brackish drinking water, J. Membr. Sci., 219 (2003) 103–112.
[133] B. Van der Bruggen and C. Vandecasteele, Modelling of the retention of uncharged molecules with nanofiltration, Water Res., 36 (2002) 1360–1368.
[134] G. Hagmeyer and R. Gimbel, Modelling the salt rejection of nanofiltration membranes for ternary ion mixtures and for single salts at different pH values, Desalination, 117 (1998) 247–256.
[135] X. Lefebvre, J. Palmeri, J. Sandeaux, R. Sandeaux, P. David, B. Maleyre, C. Guizard, P. Amblard, J.-F. Diaz and B. Lamaze, Nanofiltration modeling: a comparative study of the salt filtration performance of a charged ceramic membrane and an organic nanofilter using the computer simulation program NANOFLUX, Sep. Purif. Technol., 32 (2003) 117–126.
[136] J. Straatsma, G. Bargeman, H.C. van der Horst and J.A.Wesselingh, Can nanofiltration be fully predicted by a model? J. Membr. Sci., 198 (2002) 273–284.
[137] S. Bandini and D. Vezzani, Nanofiltration modeling: the role of dielectric exclusion in membrane characterization, Chem. Engin. Sci., 58 (2003) 3303–3326.
[138] C. van de Lisdonk, B. Rietman, S. Heijman, G Sterk and J. Schippers, Prediction of supersaturation and monitoring of scaling in reverse osmosis and nanofiltration membrane systems, Desalination, 138 (2001) 259–270.
[139] S. Bhattacharjee, J.C. Chen and M. Elimelech, Coupled model of concentration polarization and pore transport in crossflow nanofiltration, AIChE J., 47(12) (2001) 2733–2745.
[140] W.R. Bowen and A.W. Mohammad, Diafiltration of dye/salt solution by nanofiltration: prediction and optimisation, AIChE J., 44 (1998) 1799–1812.
[141] A.W. Mohammad, A modified Donnan-steric-pore model for predicting flux and rejection of dye/NaCl mixture in nanofiltration membranes, Sep. Sci. Technol., 37(5) (2002) 1009–1030.
[142] M.N. de Pinho, V. Semião and V. Geraldes, Integrated modeling of transport processes in fluid/nanofiltration membrane systems, J. Membr. Sci., 195 (2002) 1–12.
[143] V. Geraldes, V. Semião and M.N de Pinho, Flow and mass transfer modelling of nanofiltration, J. Membr. Sci., 191 (2001) 109–128.
[144] S. Sethi and M.R. Wiesner, Simulated cost comparison of hollow-fiber and integrated nanofiltration configuration, Wat. Res., 34(9) (2000) 2589–2597.
[145] A.J.P. Verberne and J.W. Wouters, H_2O, 26(14) (1993) 383.
[146] G. Binning and C.F.Q. Gerber, Atomic force microscope, Phys. Rev. Lett., 56 (1986) 930–933.
[147] W. Bowen, N. Hilal, R. Lovitt, A. Sharif and P.M. Williams, Atomic force microscope studies of membranes: force measureiment and imaging in electrolyte solutions, J. Membr. Sci., 126 (1997) 77–89.
[148] W. Bowen, N. Hilal, R. Lovitt and P. Williams, Atomic force microscope studies of membranes: Surface pore structures of Cyclopore and Anopore membranes, J. Membr. Sci., 110 (1996) 233–238.
[149] A. Bessibres, M. Meireles, R. Coratger, J. Beauvillain and V. Sanchez, Investigations of surface properties of polymeric membranes by near field microscopy, J. Membr. Sci., 109 (1996) 271–284.
[150] A.K. Fritzsche, A.R. Arevalo, M.D. Moore, V.B. Elings, K. Kjoller and C.M. Wu, The surface structure and morphology of polyvinylidene fluoride microfiltration membranes by atomic force microscopy, J. Membr. Sci., 68 (1992) 65–78.
[151] W.R. Bowen, N. Hilal, R. Lovitt and P. Williams, Atomic force microscope studies of membranes: Surface pore structures of Diaflo ultrafiltration membranes. J. Coll. Interf. Sci., 180 (1996) 350–359.
[152] W.R. Bowen, N. Hilal, R.W. Lovitt and P.M Williams, Visualisation of an ultrafiltration membrane by non-contact atomic force microscopy at single pore resolution, J. Membr. Sci., 110 (1996) 229–232.
[153] J.I. Calvo, P. Pradanos, A. Hermindez, R. Bowen,

N. Hilal, R.W. Lovitt and P.M. Williams, Bulk and surface characterization of composite UF membranes atomic force microscopy, gas adsorption–desorption and liquid displacement techniques, J. Membr. Sci., 128 (1997) 7–21.

[154] A.K. Fritzsche, A.R. Arevalo, A.F. Connolly, M.D. Moore, V. Elings and C.M. Wu, The structure and morphology of the skin layer of polyethersulfone ultrafiltration membranes: a comparative atomic force microscope and scanning electron microscope study, J. Appl. Polym. Sci., 45 (1992) 1945.

[155] A. Bottino, G. Capannelli, A. Grosso, O. Montecelli, O. Cavalleri, R. Rolandi and R. Sofia, Surface characterisation of ceramic membranes by atomic force microscopy, J. Membr. Sci., 95 (1994) 289–296.

[156] M. Elimelech, X. Zhu, A. Childress and S. Hong, Role of membrane surface morphology in colloidal fouling of cellulose acetate and composite aromatic polyamide reverse osmosis membranes, J. Membr. Sci., 127 (1997) 101–109.

[157] W.R. Bowen, N. Hilal, R.W Lovitt and C.J. Wright, A new technique for membrane characterisation: direct measurement of the force of adhesion of a single particle using an atomic force microscope, J. Membr. Sci., 139 (1998) 269–274.

[158] W.A. Ducker, T.J. Senden and P.M. Pashley, Measurement of force in liquid using a force microscopy, Langmuir, 8 (1992) 1831–1836.

[159] N. Hilal and W.R Bowen, Atomic force microscope study of the rejection of colloids by membrane pores, Desalination, 150 (2002) 289–295.

[160] W.R. Bowen, N. Hilal, R.W Lovitt and C.J. Wright, Characterisation of membrane surfaces: direct measurement of biological adhesion using an atomic force microscope, J. Membr. Sci., 154 (1999) 205–212.

[161] W.R. Bowen and T.A. Doneva, Atomic force microscopy studies of nanofiltration membranes: Surface morphology, pore size distribution and adhesion, Desalination, 129 (2000) 163–172.

[162] A.W. Mohammad, N. Ali and N. Hilal, Investigating characteristics of increasing MWCO polyamide nanofiltration membranes using solutes rejection and atomic force microscopy, Separ. Sci. Technol., 38(6) (2003) 1307–1327.

[163] A.W. Mohammad, N. Hilal and M. Abu Seman, A study on the producing composite nanofiltration membrane with optimised properties, Desalination, 158 (2003) 73–78.